RESEARCH

The effects of applying different bias voltages and phase differences on performance of an asymmetric surface dielectric barrier discharge; an experimental investigation

H. Mahdavi[1] · F. Sohbatzadeh[1]

Abstract

In the present research, the performance of the electrohydrodynamic force in an asymmetric surface dielectric barrier discharge actuator has been investigated at different bias voltages. The effects of DC, AC plus DC (DC-offset), and sinusoidal bias voltages on the force generation have been studied through measuring the electric wind velocity profiles, surface potential, and electric field. The results showed that applying DC and DC-offset biases to the lower electrode instead of connecting it to the ground in a typical case increased the charge deposition on the dielectric surface and consequently reduced the electrohydrodynamic force generation. This effect was also observed in case of exchanging these voltages with AC sinusoidal voltage of the upper electrode. In addition, as a new idea, two-phase shifted AC voltage was applied to the electrodes and the resulting changes have been studied. The obtained results at $180°$ phase difference were very noticeable and showed 46% improvement in the maximum velocity of the induced flow relative to the grounded electrode with the same input power. Using this technique, a certain wind velocity can be obtained at relatively lower voltages and input powers compared to the conventional case of grounding the lower electrode. Such a capability is significant in aerodynamic applications, where applying large values of the high voltages may disturb the operational systems.

Keywords Asymmetric surface dielectric barrier discharge · Electric wind · Electrohydrodynamic force · Surface potential

Introduction

In the recent decades, atmospheric pressure plasma especially the dielectric barrier discharge (DBD), which consists of a dielectric material between the electrodes to form a stable and uniform discharge, has been known in a variety of applications such as surface treatment, air pollution control for the removal or decomposition of pollutant particles, sterilization, and medical area [1–6]. Recently, DBD has been employed in a new specific structure that was suggested by Roth [7]. This is an asymmetric surface dielectric barrier discharge (ASDBD) in which the plasma extends over a

✉ F. Sohbatzadeh
   F.sohbat@umz.ac.ir

   H. Mahdavi
   Hoda.mahdavi65@gmail.com

[1] Department of Atomic and Molecular Physics, Faculty of Basic Sciences, University of Mazandaran, Babolsar, Mazandaran 47416-95447, Iran

dielectric surface that covers the lower electrode. The upper electrode, which is placed asymmetrically with respect to the lower one, is exposed to air and powered by an AC high voltage, while the buried electrode is grounded. As the result of plasma-accelerated ion interactions with the air neutral molecules, the momentum transfers to the surrounding air and a secondary flow, which is called the ionic wind or electric wind, will be induced. The effect of ASDBD in injecting momentum to the flow is noticeable in aerodynamic flow control applications, so a lot of experimental and numerical studies have been done to improve its operation efficiency [8–12]. Porter et al. [13] investigated the phenomenology of the momentum transfer to air by measuring the temporal and time averaged body force. Mahdavi et al. [14] have done another study in body force production by introducing a new supplementary theory named nonlinear body force. Morea et al. [15] enhanced the mechanical efficiency of the electrical wind by optimizing the corona discharge properties. Corke and Thomas [16, 17] also made valuable efforts to optimize the ASDBD performance. Since the mechanism of the surface DBD plasmas is mainly determined by the

charges deposited on the dielectric surface, some researchers have studied its effect on the EHD force performance. Font et al. [18] measured the surface potential distribution of the ASDBD by a V-dot probe. Enloe et al. [19] and Nicolas et al. [20] also used the same technique for the surface DBD to find out the electric field structure in the plasma and study the spatiotemporal evolution of the surface potential at low pressures. Recently, Cristofolini et al. [21] have investigated the effect of charge surface deposition on the induced flow by using three different geometrical configurations. Young et al. also [22] designed thin foil, blade, wire, and copper mesh configurations of the upper electrode and drove it by an AC high voltage and DC biases to investigate the relevancy of surface potential to the mechanical characteristics.

Studies indicate that the electrical characteristics of the ASDBDs certainly affect the electric wind production. Benard et al. [23] compared the effects of sinusoidal, square, positive and negative ramp input voltage waveforms on the body force production. Abe et al. [24] also investigated the role of the negative and positive part of the sinusoidal wave and its corresponding slop in momentum transfer. In 2015, Borghi et al. [25] measured the electric wind velocities of the ASDBD, which was supplied by a high-voltage–high-frequency multilevel generator. The induced flow of the ASDBD, which was driven by ns-HV pulses superimposed on a DC or low frequency sinusoidal voltage, was investigated by Opaits et al. [26]. Recently, Yon et al. [27] studied the effects of applying DC bias voltage to the exposed electrode on the induced EHD force, while the lower electrode was connected to AC sinusoidal voltage. In this paper, we also studied the effects of the input electrical parameters on the ASDBD performance.

In the first part of the paper, we investigated the effects of applying different bias voltages to the lower electrode instead of connecting it to the ground in a typical structure. (The AC voltage is applied to the upper electrode and the lower one is grounded.) The bias voltages were DC voltage and a new type of the voltage waveform, named DC-offset, which is in fact an AC sinusoidal voltage superimposed to a DC bias. The studies were done through measuring the electric wind velocity profile, the surface potential and the electric field at different distances form the upper electrode edge. Further experiments were carried out by exchanging the applied DC, DC-offset, and ground voltages of the lower electrode with the AC sinusoidal voltage of the upper one.

Since the results of applying DC and DC-offset voltages to the electrodes in our experiments indicated no significant improvement in the induced electric wind velocity, we considered an alternative case of applying voltage. In this case, we studied the effect of applying an AC sinusoidal voltage to the lower electrode, which was synchronized, with the sinusoidal voltage applied to the upper one. For this purpose, we designed a new switching circuit using a microcontroller element to produce two independent sinusoidal voltages with an adjustable phase difference. The experimental results of applying two sinusoidal voltages with zero phase difference to the upper and lower electrodes encouraged us to study the phase difference of two AC voltages as a new parameter, which to the best of our knowledge has not been studied yet in the ASDBD performance. We carried out similar measurements of the previous cases for different values of the phase differences.

This article is organized as follows:

In Sect. 2, the methods and apparatuses of the experimental measurements are explained, in Sect. 3 the results of the experiments concerning applying DC/DC-offset bias voltages to the lower electrode, exchanging the upper and lower electrode voltages and applying the phase difference between the voltages of the electrodes are presented. In the last section, the conclusions of the experiments are discussed.

Materials and measurement methods

Experimental setup

Two aluminum foils with 0.08 mm thickness and 6 cm length were used as the electrodes of the ASDBD. The upper electrode was exposed to air, and the lower one was covered by a 2 mm PMMA plate as the dielectric layer. To prevent unwanted discharges, the lower electrode was encapsulated by another 3 mm PMMA plate, as shown in Fig. 1. The width ratio of the upper and lower electrodes was equal to $\frac{1}{3}$, and they were placed asymmetrically with zero overlap distance.

In the first part of the experiments, three kinds of high-voltage waveforms were used: An AC sinusoidal voltage, a DC voltage, and an AC sinusoidal voltage superimposed to a DC one to make a DC-offset waveform. In order to investigate the role of applying DC and DC-offset voltages to the lower electrode instead of connecting it to the ground, the AC sinusoidal voltage at the frequency and voltage of 5.5 kHz and 19 kV_{pp} was applied to the upper electrode and the DC and DC-offset voltages from 0 to $\pm$ 9 kV were applied to the lower one. Moreover, to study the effects of exchanging the upper/lower electrode voltages on the EHD force performance (the electric wind velocity, thrust force, surface potential and electric field), we applied the sinusoidal voltage to the lower electrode and connected the upper electrode to one of these three cases: ground, DC and DC-offset voltages. In this case, to shield the DC circuit from the sinusoidal AC discharge currents we put the electrode in series with a 1 MΩ resistor. Furthermore, to isolate the AC power supply and the SDBD from DC signals, the upper
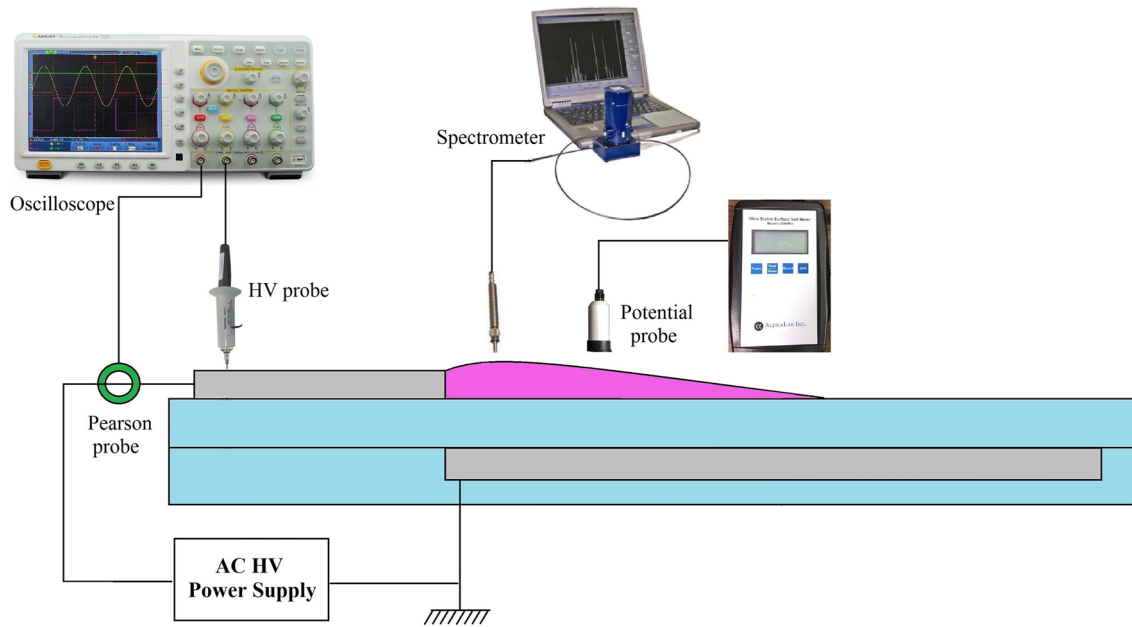
Fig. 1 Schematic picture of the ASDBD structure

electrode is grounded through two series capacitors, which is shown in Fig. 2.

The voltage and current measurements were carried out by using a high-voltage probe (Tektronix P6015A.Tektronix, Inc.) and a Pearson probe (Pearson Electronics model 4100), which were recorded by a digital oscilloscope (Tektronix DPO, 2012, Tektronix, Inc.).

Surface potential

An electrostatic voltmeter (USSVM model made by α Lab. Inc) was used to measure the average potential on the dielectric surface. The probe was held at 2.54 cm from the dielectric surface, and the potential was measured across the width of
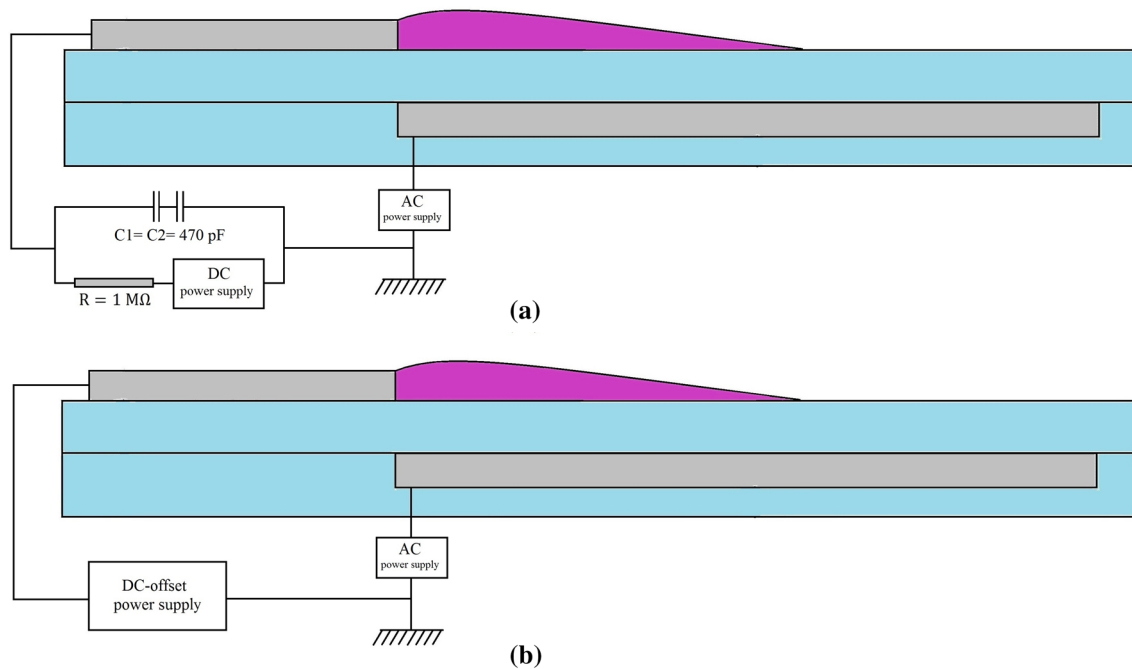

Fig. 2 A schematic picture of applying DC (**a**) and DC-offset (**b**) voltages to the upper electrode

the covered electrode. Plasma was run for 30 s, and immediately after it was turned off, the potential was measured on the dielectric surface. For each case, the potential measurements were conducted for four times and the average results were reported. The voltmeter probe also measures the electric field above a charged insulator plate with no ground plane under it. Therefore, we estimated the value of the electric field in the region downstream of the covered electrode width.

Electric wind velocity measurement

The average velocity of the electric wind was measured by using the pitot tube technique which is a usual procedure to measure the velocity of an incompressible flow. The pitot tube used in the measurements connected to a micro manometer of Kimo Inc. model MP110, from -1000 to 1000 Pa with 1 Pa resolution. Since a commercial Pitot tube is made of stainless steel, it may lead to spark at distances near the discharge surface, so we used a glass capillary tube with the inner diameter of 0.5 mm to measure the total pressure. A 2D x–z positioner with 0.01 mm accuracy was employed to displace the glass tube along the horizontal and vertical axes. The differential pressure read from the micro manometer was inserted in the velocity relation of our pitot tube to calculate the electric wind velocity.

Experimental results

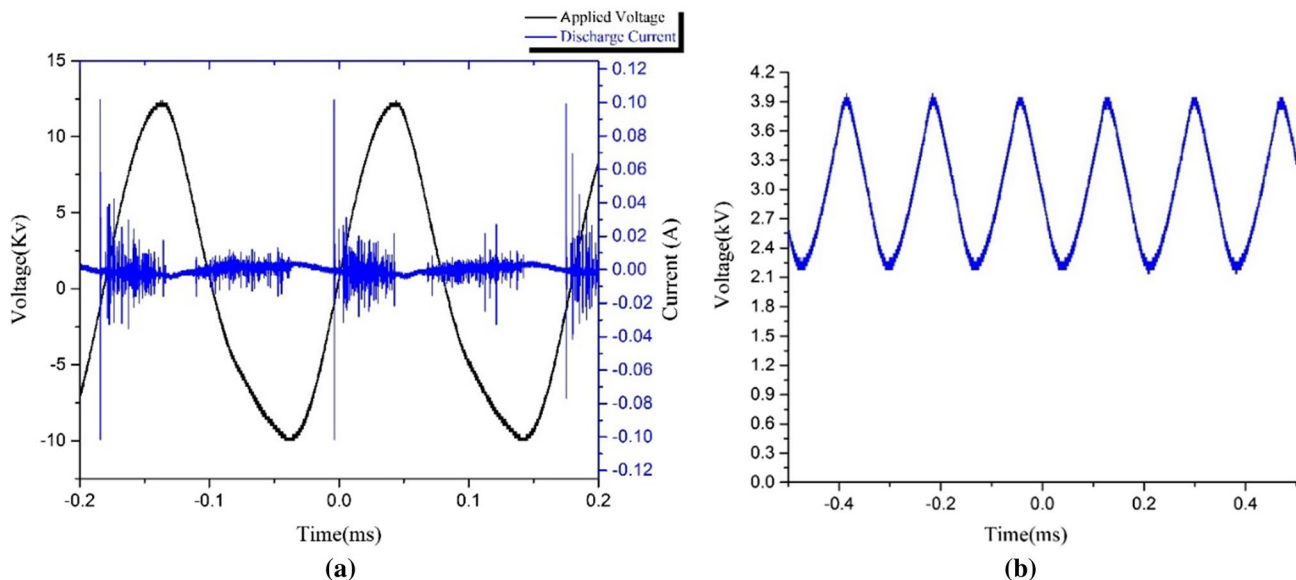### Applying DC and DC-offset voltages to the lower electrode

In order to examine the effects of applying different voltage waveforms to the electrodes on the characteristics of the

EHD force, three types of voltages were utilized. The DC voltage and a new type of the voltage waveform, called DC-offset, were applied to the lower electrode, while the upper electrode was powered by an AC sinusoidal voltage. The amplitude and frequency of the AC voltage were fixed at 19 kV_{pp} and 5.5 kHz, respectively. The $+/-$ DC-offset waveform is made of the superposition of an AC waveform with a $+/-$ DC one. The mean value of the $+/-$ DC and DC-offset waveforms varied from 0 to $\pm$ 9 kV, where the case of DC-offset waveform also included a sinusoidal AC voltage with 0 to 2.5 kV_{pp} at the frequency of 5.5 kHz. The typical voltage characteristics of these waveforms are shown in Fig. 3.

Investigations were carried out by measuring the electric wind velocity, the dielectric surface potential and the electric field. The results of these experiments are discussed below.

The electric wind velocity profile

Figure 4 indicates the measurement results of applying DC and DC-offset voltages to the lower electrode. In order to investigate the effects of these bias voltages the results of connecting the lower electrode to the ground (typical case) were also shown. We observed that the electric wind velocity decreased by increasing the DC and DC-offset voltages of both positive and negative polarities. This reduction for the positive polarity of the DC voltages was more considerable than the negative polarity. In contrast, for the case of the DC-offset voltages, the velocity fluctuations were significant in the negative polarity and they were relatively small in the positive one. The negative polarity of DC-offset voltage also induced higher electric wind velocities with more extension than the positive one in all distances downstream of the upper electrode. The average of the electric wind velocity

Fig. 3 Voltage characteristics of the sinusoidal (**a**) and DC-offset (**b**) voltages
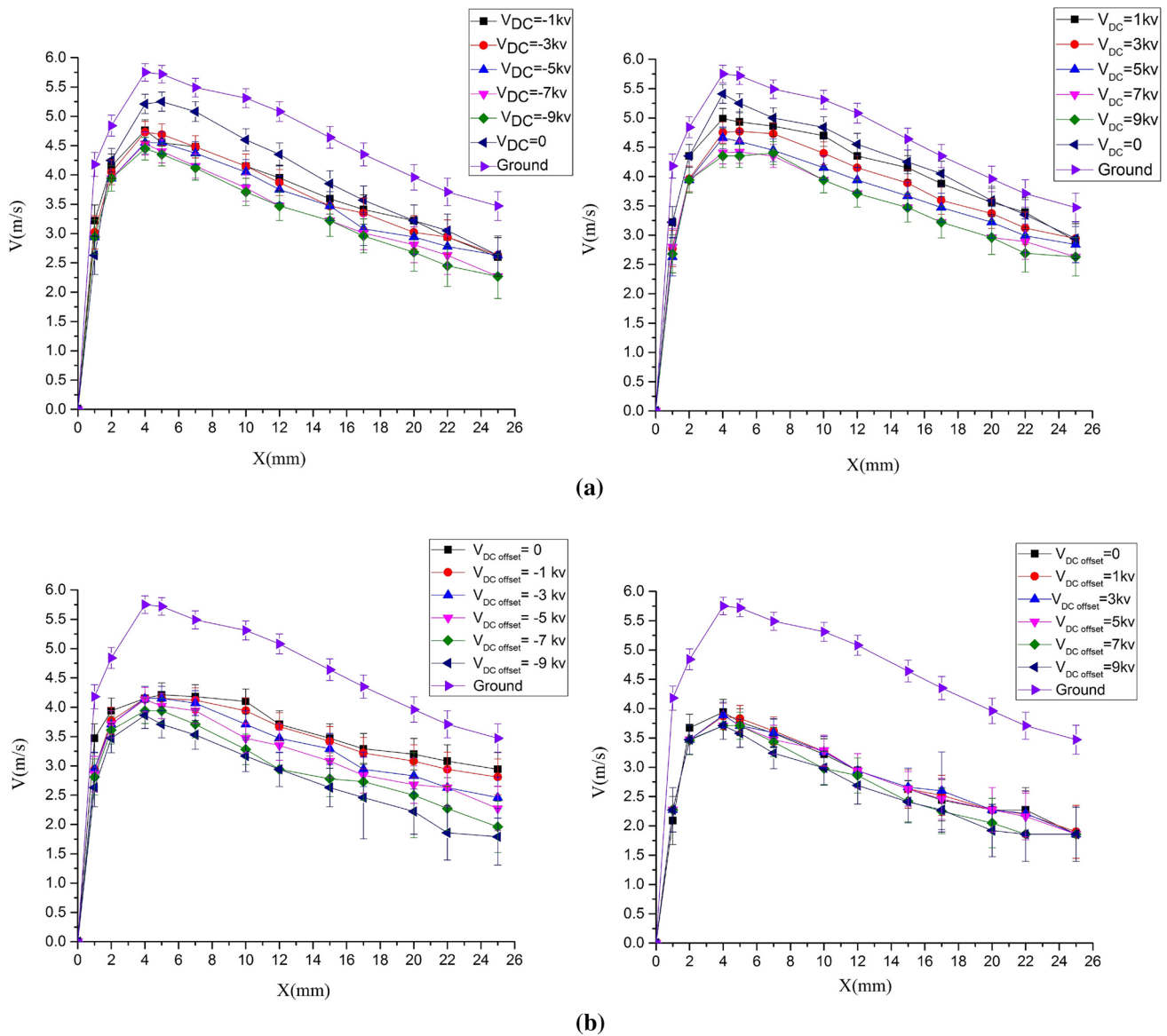
Fig. 4 The electric wind velocity profile for the case of applying (a) DC/ground and (b) DC-offset/ground voltages to the lower electrode and AC sinusoidal voltage to the upper one

and the maximum velocity for each bias voltage are available in Tables 1 and 2.

Analyzing the results of measurements reveals that applying the DC voltages to the lower electrode produce greater electric wind velocities than the DC voltages with an AC component. However, grounding the lower electrode resulted in the best efficiency of EHD force generation relative to other bias voltages.

We should note that, from the theoretical point of view, it is expected that the zero DC/DC-offset bias and the grounded electrode cases should be the same and produce the similar velocity profiles, but a major difference is seen

Table 1 The average and maximum velocities of positive/negative DC-offset bias voltages in downstream of the exposed electrode edge

$V_{DC\text{-}offset}$(kV)	− 1	− 3	− 5	− 7	− 9	1	3	5	7	9
Velocity(m/s)										
$V_{average}$	3.52	3.36	3.25	3.04	2.86	2.89	2.89	2.85	2.52	2.69
V_{max}	4.15	4.15	4.13	3.94	3.86	3.87	3.89	3.71	3.71	3.71

Table 2 The average and maximum velocities of positive/ negative DC bias voltages in downstream of the exposed electrode edge

V_{DC}(kV)	− 1	− 3	− 5	− 7	− 9	1	3	5	7	9
Velocity(m/s)										
$V_{average}$	3.75	3.98	3.587	3.43	3.38	4.11	3.87	3.71	3.56	3.59
V_{max}	4.76	4.73	4.55	4.53	4.45	4.99	4.77	4.65	4.41	4.35

between the results. It may be due to the possibility that the zero DC/DC-offset voltage was not exactly zero and a slight ripple was observed in these voltage waveforms.

The surface potential and electric field measurements

In Figs. 5 and 6, the average surface potential measurements are shown. It is clearly observed that increasing the DC and DC-offset voltages enhances the magnitude of the surface potential for both positive and negative polarities.
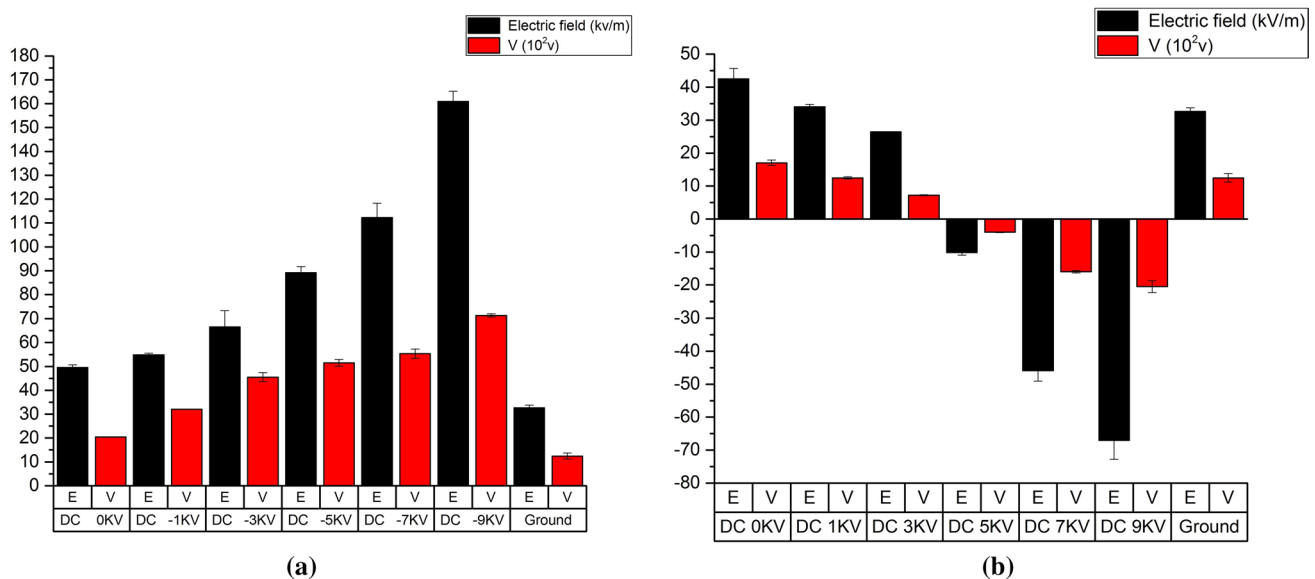
The comparison of the surface potential and the electric wind velocity profiles shown in Fig. 4 indicates that the charge build up on the dielectric surface, weakens the EHD force generation [11]. This is in agreement with the previous studies, which had claimed that increasing the EHD force needs the charge accumulation on the dielectric surface to decrease [28–31]. During recent years, the authors have examined different procedures to reduce the charges on the dielectric surface, e.g., using materials with high permittivity (i.e., a large ε value) [28] was the first evidence that reduction of charges on the dielectric surface is a way for improving the momentum transfer of the actuator. Considering a new DBD structure in which just a part of the lower electrode was covered by the dielectric material [29, 30] or utilizing special coatings to increase charge mobility was the other ideas to decrease the surface charges [31].

Applying the DC or DC-offset bias voltages to the lower electrode increases the surface potential values up to four times of the ground case values and resulted in lower electric wind velocities. As it is obvious in Fig. 4, the maximum velocity, which is about 6 m/s, is generated when the lower electrode is grounded.

The sign of the surface potential, when we applied the sinusoidal voltage to the exposed electrode and connected the other one to the DC voltages, became positive for the negative polarity and contrarily negative for the opposite polarity voltages above 3 kV. Interestingly the same results were obtained in the case of applying DC-offset voltages even for the voltage value above which the potential became negative. In the case of connecting the lower electrode to the ground, the potential was positive and lower than the values for the DC and DC-offset voltages.

The electric field measurements were done by the same probe in downstream region of the encapsulated electrode width. Since the width of the exposed and covered electrodes was 10 mm and 30 mm, respectively, the electric field was measured at 30–60 mm downstream of the exposed electrode

Fig. 5 The surface potential and electric field in the case of applying AC sinusoidal voltage to the upper electrode and the negative (**a**)/positive (**b**) DC voltages and ground to the lower electrode
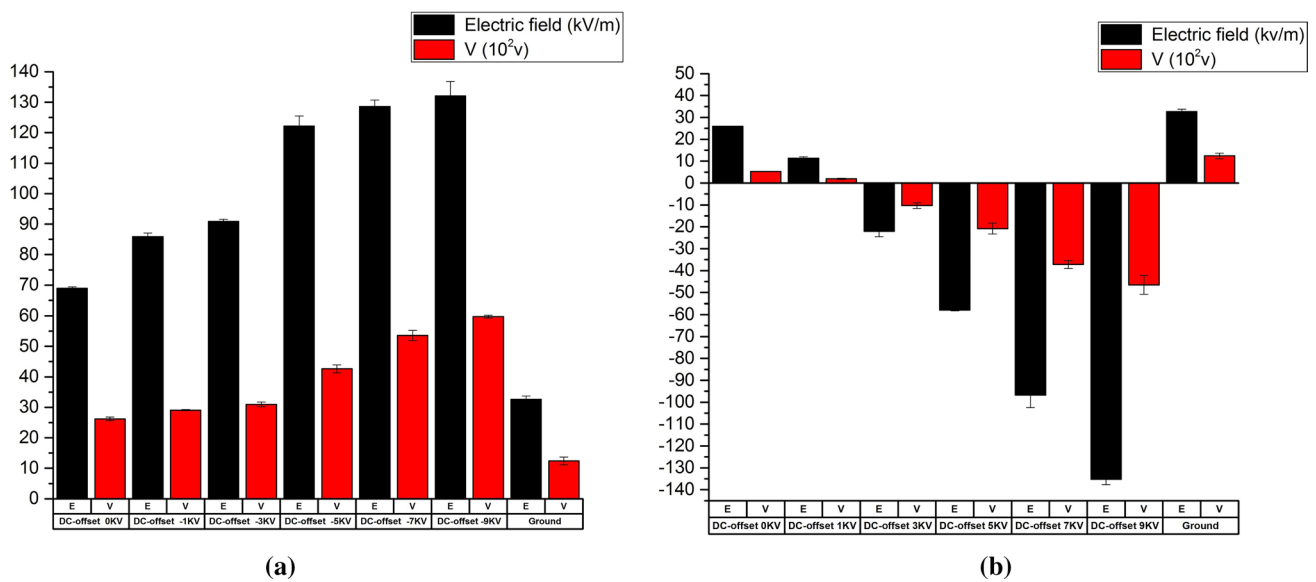
Fig. 6 The surface potential and electric field in the case of applying AC sinusoidal voltage to the upper electrode and the negative (**a**)/positive (**b**) DC-offset voltages to the lower electrode

lower edge. A noticeable point was that although the plasma extends only a few millimeters (maximum extension up to 10 mm), the measured electric field strength, even at the distance 30 mm far from it, was nonzero.

The sign and magnitude of the electric field were similar to the surface potential behavior in all cases of applying DC, DC-offset, and ground voltages.

Exchanging the applied voltages of the lower and upper electrodes

Further experiments were carried out by exchanging the voltages of the upper and lower electrodes in the previous section and investigating its effects on the EHD force production, surface potential and electric field. Thus, we applied the AC sinusoidal voltage to the lower electrode and the DC, DC-offset and ground voltages to the upper one. The results of the measurements are discussed in the following sections.
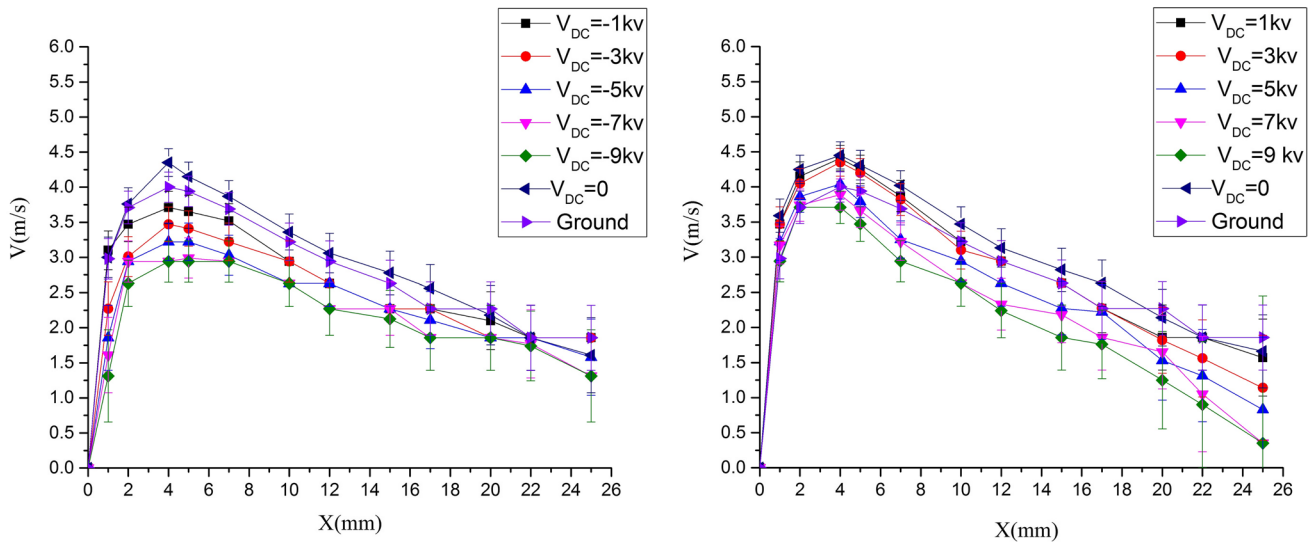
The electric wind velocity profile

The results of the electric wind velocity measurements in the case of applying DC, DC-offset and ground voltages to the upper electrode and connecting the lower one to the AC sinusoidal voltage are shown in Figs. 7 and 8.

It is inferred from the figures that by increasing the DC and DC-offset voltages of both positive and negative polarities, the electric wind velocities decrease. This reduction was too significant for the DC-offset voltages in both magnitude and extension of the induced velocities and especially for the negative ones such that the

maximum velocity was about 2 m/s. In the case of positive DC voltages, the electric wind velocities decayed fast away from the upper electrode edge, whereas the DC negative polarity produced greater wind velocities than the positive one at those points. Considering the velocity profiles also revealed that in the region near the exposed electrode edge (discharge zone), the applied DC and DC-offset voltages had little effects on the wind velocities, since the different values of the DC and DC-offset voltages had nearly the same velocity profiles. In fact, in this area because of good electrical conductivity of the plasma the applied DC and DC-offset biases give rise to a little voltage drop that causes a less effect on the EHD force [27]. However, downstream of the discharge area the influences of these voltages can be obviously seen. It is also inferred from the velocity measurements that the drift of charged particles under the effect of DC electric fields in downstream regions were stronger than that of the DC-offset biases whether they applied to the upper or to the lower electrode.

In 2015, a similar study was reported by Yan et al., in which the effect of a DC bias on the EHD force induced by an AC SDBD actuator was investigated [27]. They applied the +/− DC voltages to the upper electrode and connected the lower one to an AC power supply. Based on [27], beyond the AC discharge plasma area, the negative DC bias leads to an increase in the induced ionic wind velocity, while the positive DC bias causes a significant decrease. There is a good agreement between the measurement results of our paper and that of [27] for the positive DC polarities, whereas for the negative DC bias, a discrepancy in the results was observed. This may be related to the differences

Fig. 7 The electric wind velocity profiles in the case of applying AC sinusoidal voltage to the lower electrode and positive/negative DC and ground voltages to the upper electrode
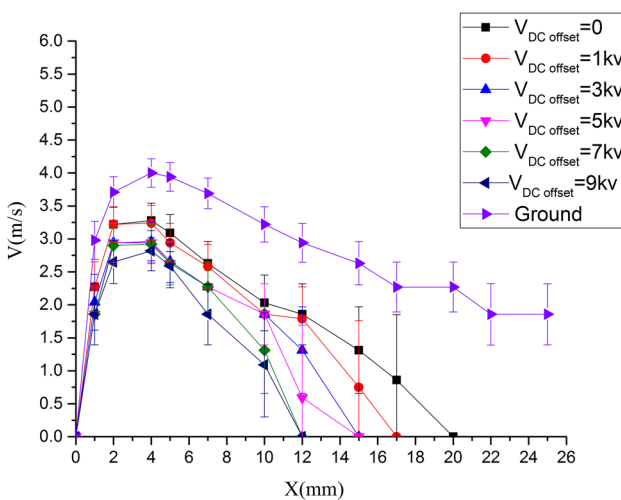
Fig. 8 The electric wind velocity profile in the case of applying AC sinusoidal voltage to the lower electrode and positive DC-offset and ground voltages to the upper one

in electrical circuit design and the characteristic parameters of two ASDBDs.

The surface potential and electric field measurements

The surface potential measurements, which are depicted in Figs. 9 and 10, showed that applying bias voltages to the upper electrode also increased the surface potential in terms of increasing voltages. Considering the surface potential measurement results indicated that the case of applying ground voltage to the upper electrode had the lowest value

of the potential and electric field compared with the bias voltages.

The sign of the surface potential can be an indication of the charge type deposited on the dielectric surface and contributes to the EHD force production via discharge memory effects. The sign of the potential and electric field in the experiments of this section almost depended on the polarity of the applied DC and DC-offset voltages and it was positive for the ground case. For the positive DC/DC-offset voltages, it was always positive and for the negative DC voltages above −1 kV, it was negative.

### The effects of phase differences between the applying voltages

Experimental setup

The third case of applying voltages that we considered was applying an AC sinusoidal voltage to the lower electrode at the same frequency of the upper one. The phase difference between the voltages was an important parameter in this case. To produce and control this parameter, we designed a new switching circuit, which includes a microcontroller, model PIC16F887, to produce two independent sinusoidal voltages with an adjustable phase difference for a wide range of frequencies (1–40 kHz, see figure A1 in the appendix). Since the existing of noises is a key parameter in the design of high-voltage circuits, we used PIC microcontroller series, which have a large resistance against noises. In this circuit, two signals are required so we exploited a processor that has two PWM

(a)

(b)
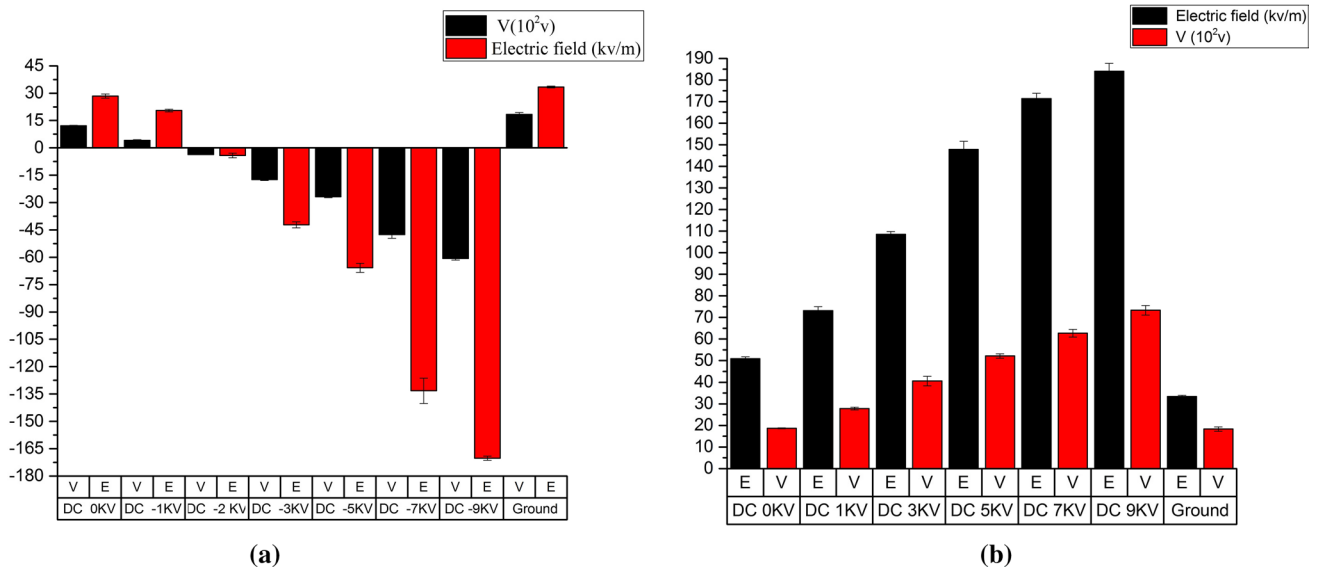
Fig. 9 The surface potential and electric field for the case of applying AC sinusoidal voltage to the lower electrode and the negative (**a**)/positive (**b**) DC and ground voltages to the upper electrode
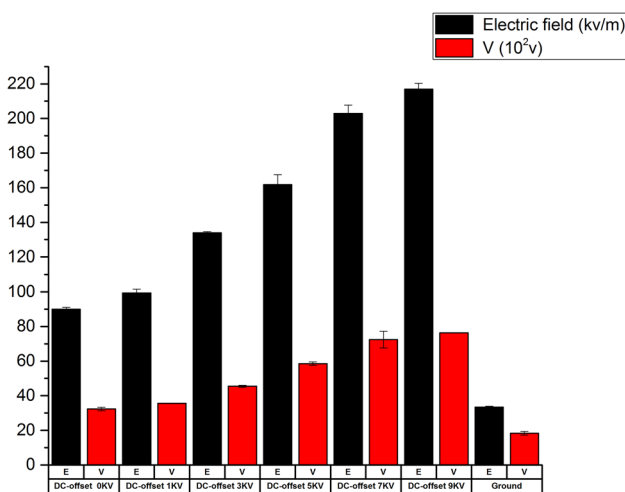
Fig. 10 The surface potential and electric field for the case of applying AC sinusoidal voltage to the lower electrode and the positive DC-offset and ground voltages to the upper electrode

modules. These modules should have the capability to apply time delay with respect to each other up to 180° phase difference.

The experiments were carried out by utilizing the same structure of the ASDBD explained in Sect. 2–1. We applied the sinusoidal voltages with three different values of phase differences to the upper and lower electrodes, i.e., $\Delta\phi = 0°$, $\Delta\phi = 90°$ and $\Delta\phi = 180°$ (see Fig. 11). To investigate the effects of phase difference between two applying AC voltages, the frequencies of them must be equal. In the experiments of this section according to new circuit design, the frequencies were fixed at 26 kHz.

The measurement results

In order to study the effects of phase difference between the applied voltages on the characteristics of the EHD force, the electric wind velocity measurements were carried out by using the pitot tube probe described in Sect. 2–3.

For the case of $\Delta\phi = 0°$, two synchronized sinusoidal voltages at the same frequencies and voltage amplitudes were applied to the electrodes. As it was expected by increasing the voltages, no plasma sheet was formed between the electrodes. Since the upper and lower electrodes have the same potential, the potential difference between two electrodes is always zero, and the electric field is not strong enough to initiate an electrical breakdown. Therefore, the electric wind velocity measurements indicated no wind production.

Phase difference cases of $\Delta\phi = 90°$ and $\Delta\phi = 180°$ were examined at equal input switching powers with the voltages $V_{1s} = V_{2s} = 8$ V and the currents $I_{1s} = I_{2s} = 0.16$ A. The corresponding values of output high voltages, V_{1pp} and V_{2pp}, of 8.2 kV and 6.8 kV were applied to the lower and upper electrodes, respectively.

The results of the electric wind velocity measurements are shown in Fig. 12. In order to investigate the effects of the considered phase differences, the measurement results of the typical structure of an ASDBD, where the lower electrode was grounded and the upper one was powered by a sin voltage (with $V_{pp} = 6.8$kV), were shown in this figure, too.
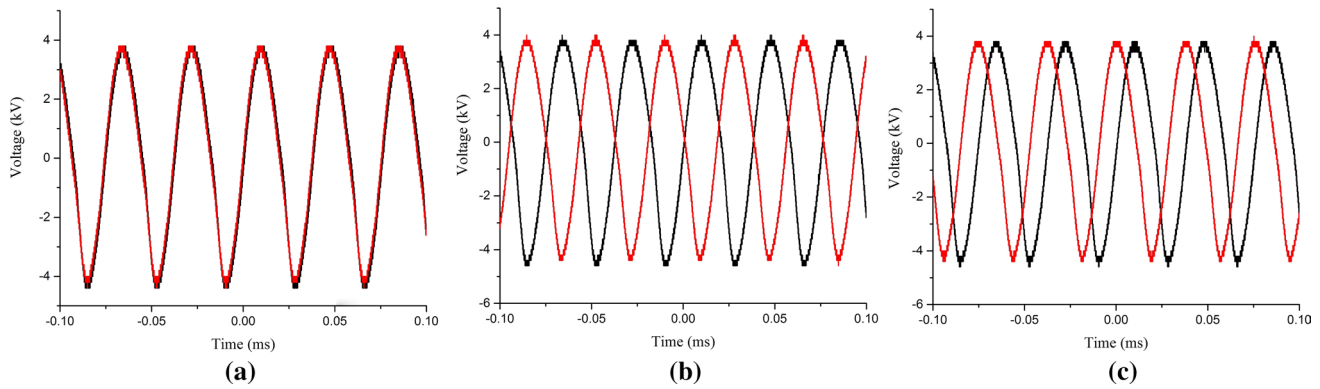
Fig. 11 The voltage–time characteristics of the applied voltages to the upper and lower electrodes with (**a**) zero, (**b**) 180° and (**c**) 90° phase difference

The electric wind velocity measurements indicated that the magnitude and the extension of the wind velocity induced by applying 90° phase difference to the voltages of the upper and lower electrodes were obviously smaller than the cases of $\Delta\phi = 180°$ and ground. However, the results of applying a sinusoidal voltage to the lower electrode with $\Delta\phi = 180°$ with respect to the upper one were so noticeable. In this case, a flow induction with considerably higher velocities than the ground case was obtained, such that the maximum wind velocity of the 180° phase difference was about 3.8 m/s, whereas it was 2.6 m/s for the ground case. This 46% improvement in the wind velocity is very exciting, which can be beneficial in the flow control applications. Employing the same input power of the cases with phase difference for the typical structure led to a greater high voltage. This apparently would alter the discharge mode and may disturb the performance of the actuator.

Furthermore, we applied the AC sinusoidal voltages with the same peak-to-peak amplitude values to the upper and lower electrodes. V_{1pp} and V_{2pp} are set at 7.6 kV, where the switching voltages and currents are $V_{1s} = 6.8$ V, $V_{2s} = 8$ V, $I_{1s} = 0.21$ A and $I_{2s} = 0.16$ A. The electric wind velocity measurements for $\Delta\phi = 90°$ and $\Delta\phi = 180°$ cases are reported in Fig. 13. The results of the electric wind velocity measurements in this case showed the similar behavior with the previous case of equal input power. It was seen that the electric wind velocity generated by 180° phase difference between voltages was greater than that of the ground case and the induced electric wind by $\Delta\phi = 90°$ was noticeably smaller than ground and $\Delta\phi = 180°$ cases.

Another important quantity that should be considered as the fixed parameter to analyze the performance of the plasma actuator is the electric wind velocity. Therefore, we chose two specific velocities at a certain point and compared the required high voltages and input powers of $\Delta\phi = 180°$ and ground cases. For this purpose, the required electrical values to generate the wind velocities of 3.75 m/s and 2.94 m/s

at 4 mm downstream of the upper electrode edge, for both cases were measured and presented in Tables 3 and 4.

Investigating the values in Tables 3 and 4 indicates that for both values of the electric wind velocities, applying 180° phase difference between the voltages of the upper and lower electrodes leads to 10% reduction in the amount of high voltages and about 30% decrease in the input switching powers with respect to the ground case. This means that by applying $\Delta\phi = 180°$ between the voltages of two electrodes greater wind velocities and extensions can be obtained by consuming lower values of input powers and high voltages than the typical case.

This result is valuable in flow control applications because applying large values of the high voltages may disturb the electrical operational systems. Therefore, reduction in the applied high-voltage amplitudes is very important in practical applications.
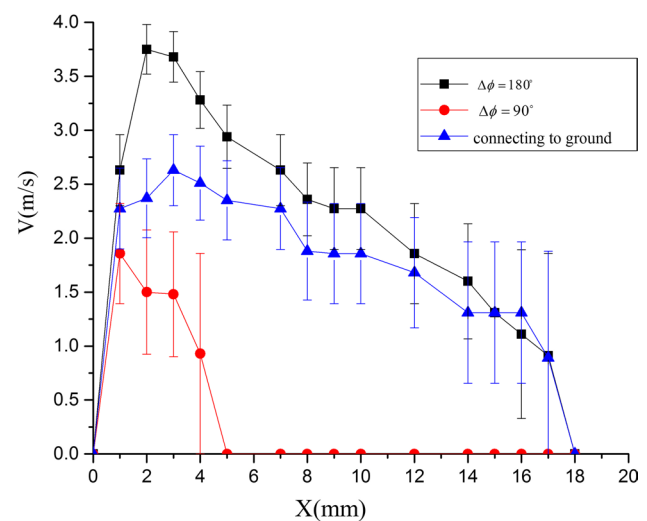
Fig. 12 The electric wind velocity profile for the typical case of applying voltage and 90°, 180° phase differences between the voltages of the electrodes in equal switching voltages
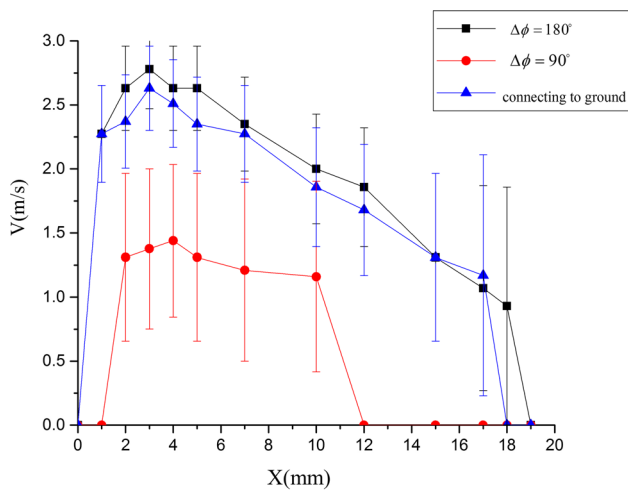
Fig. 13 The electric wind velocity profile for the typical case of applying voltage and 90°, 180° phase difference between the electrode voltages by applying equal high voltages

Table 3 The values of electrical parameters for $V = 3.75$ (m/s) in the cases of $\Delta\phi = 180°$ and grounding the lower electrode

$V_1 = 3.75$ (m/s)	$I_{switching}$ (A)	$V_{switching}$ (V)	$V_{pp\text{-}upper/lower\ electrodes}$ (kV)
$\Delta\phi = 180°$	0.17	9	8.4
Connecting the lower electrode to ground (1)	0.22	10	9.5

Table 4 The values of electrical parameters for $V = 2.94$ (m/s in the cases of $\Delta\phi = 180°$ and grounding the lower electrode

$V_2 = 2.94$ (m/s)	$I_{switching}$ (A)	$V_{switching}$ (V)	$V_{pp\text{-}upper/lower\ electrodes}$ (kV)
$\Delta\phi = 180°$	0.13	7	6.4
Connecting the lower electrode to ground (1)	0.18	8	7.5

Fig. 14 The electric field and surface potential measurement results for different values of the applied high voltages in the cases of table
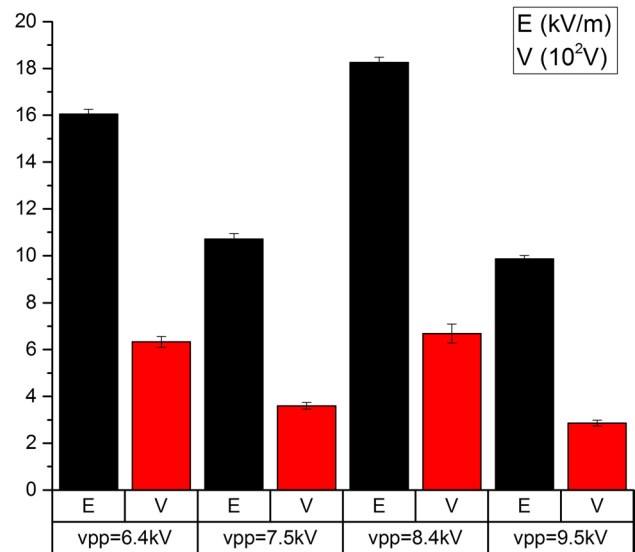
As the last part of the experiments, the surface potential and the electric field were also measured, and the results are depicted in Fig. 14. The measurement results indicate that applying 180° phase difference to the upper and lower electrode voltages leads to higher values of the surface potentials and electric fields relative to the typical case. Since the electrodes have equal peak-to-peak voltages with opposite polarities in the case of $\Delta\phi = 180°$, the magnitude of potential difference and consequently the electric field between the electrodes increase. This also leads to the enhancement of the surface charge deposition by increasing voltages.

Conclusions

In the first part of this paper, the effects of applying DC and DC-offset voltage waveforms to the lower electrode on the EHD force performance was investigated. The reverse case of applying voltage was also studied, where the voltage of the lower electrode was exchanged with the AC sinusoidal waveform of the upper one. The electric wind velocity measurements indicated that applying these bias voltages to the lower electrode has reduced the EHD force generation compared to the case of connecting it to the ground, which can be found in a typical structure of an ASDBD. Moreover, the experimental investigations showed major differences in the values of the electric wind velocities with exchanging voltages. The velocity measurement results showed that: (1) Applying the sinusoidal voltage to the upper electrode and grounding the lower one generated the maximum electric wind velocity (about 6 m/s) among all the cases, where DC/DC-offset voltage had been applied to the upper/lower electrodes. (2) Applying DC/DC-offset voltage and ground to the covered electrode, when the sinusoidal voltage was applied to the exposed one, produced higher electric wind velocities compared to the reverse cases. (3) Comparing the results of applying DC and DC-offset voltage to one of the upper/lower electrodes showed that the DC voltage induced higher wind velocities compared to the DC-offset voltage. (4) By connecting the exposed electrode to the sinusoidal voltage and the covered one to the DC voltages, an electric wind with higher velocities was induced at positive polarities comparing to the negative ones. In contrast, for the case of applying DC-offset voltages, the electric wind velocity and its extension for the negative polarity would be greater

than that of the positive one. (5) In all cases of applying DC/DC-offset voltages, the electric wind velocity was decreased by increasing voltage. (6) The effects of applying different values of DC/DC-offset voltage to either of the lower or upper electrodes were small in the region close to the edge of the upper electrode and became more considerable as the distant was increased.

The order of the measured dielectric surface potential was comparable with the order of the applied voltages. It can be concluded that charge deposition on the dielectric surface can modify the external electric field and consequently the EHD force generation. Comparing the results of surface potential with those obtained from the electric wind velocity measurements indicated that increasing the surface potential would lead to the reduction in the electric wind velocity. The electric field measurements in downstream of the covered electrode width indicated that the electric field strength, even at regions far from the plasma extension, was nonzero.

Furthermore, it was observed that exchanging the applied voltages to the upper and lower electrodes affected the sign of the surface potential and the electric field. When an AC sinusoidal voltage was applied to the lower electrode and a DC/DC-offset voltage to the upper one, the sign of the surface potential and the electric field changed corresponding to the polarity of the latter voltages. In case of applying an AC sinusoidal voltage to the upper electrode and connecting the lower one to a negative DC/DC-offset voltage or to the ground, both of the surface potential and the electric field were positive at all voltages. In contrast, for the positive polarity of the DC/DC-offset voltages above 1 kV or 3 kV, they became negative. In the ground case, it was always positive regardless of grounding either of the lower or upper electrodes.

In the second part of the paper, the electric wind production in the case of applying $180°$, $90°$, and zero phase differences to the voltages of the upper and lower electrodes was investigated, and the resulting changes were scrutinized. Applying two synchronized sinusoidal voltages to the electrodes caused no plasma sheet formation above the dielectric surface. At a certain value of the input (switching) power or applied high voltages, the values of the electric wind velocity induced by applying $180°$ phase difference between the voltages were considerably higher than those of the ground case and 46% increase in the velocity was observed. Moreover, the wind velocity magnitude and its extension for $\Delta\phi = 90°$ were significantly smaller than the ground case. The experiments also revealed that applying a sinusoidal voltage to the lower electrode with $180°$ phase difference with respect to the upper one could reduce the amount of the required high voltage for a specific wind velocity compared to the typical grounded case. Therefore, the main purpose of applying the phase difference between the voltages was successfully fulfilled. Decreasing the amount of the applied

high voltage to the electrode can be very influential in aeronautic applications, where the electromagnetic noises may damage the operational systems.

The results of surface potential measurements in the case of applying two sinusoidal voltages with $180°$ phase difference to the lower and upper electrodes indicated an enhancement of the charge deposition on the dielectric surface.

References

1. Kim, H.H.: Non-thermal plasma processing for air-pollution control: a historical review, current issues, and future prospects. Plasma Processes Polym. **1**, 91 (2004)
2. Xia, Y., Liu, D., Ghomi, H., Wang, W., Bi, Z., Ji, L., Wang, X., Qi, Z., Li, B.: Dynamics of ionisation wave propagation in an applied external electric field. High Volt. **1**, 90 (2016)
3. Mastanaiaha, N.: Dielectric barrier discharge (DBD) surface plasma sterilization: an in-depth study of the factors contributing to and enhancing the sterilization process. Ph.D. thesis, University of Florida (2013)
4. Sohbatzadeh, F., Mirzanejhad, S., Ghasemi, M., Talebzadeh, M.: Characterization of a non-thermal plasma torch in streamer mode and its effect on polyvinyl chloride and silicone rubber surfaces. J. Electrost. **71**, 875 (2013)
5. Gweon, B., Kim, M., Kim, D.B., Kim, D., Kim, H., Jung, H., Shin, J.H., Choe, W.: Differential responses of human liver cancer and normal cells to atmospheric pressure plasma. Appl. Phys. Lett. **99**, 063701 (2011)
6. Kaushik, N.K., Uhm, H., Choi, E.H.: Micronucleus formation induced by dielectric barrier discharge plasma exposure in brain cancer cells. Appl. Phys. Lett. **100**, 084102 (2012)
7. Roth, J.R., Sherman, D.M., Wilkinson, S.P.: Boundary layer flow control with a one atmosphere uniform glow discharge surface plasma. In: 36th AIAA Aerospace Sciences Meeting and Exhibit, Aerospace Sciences Meetings, Reno, 98-0328 (1998)
8. Orlov, D.M., Font, G.I., Edelstein, D.: Characterization of discharge modes of plasma actuators. AIAA J. **46**, 3142 (2008)
9. Boeuf, J.P., Lagmich, Y., Unfer, Th, Callegari, Th, Pitchford, L.C.: Electrohydrodynamic force in dielectric barrier discharge plasma actuators. J. Phys. D Appl. Phys. **40**, 652 (2007)
10. Forte, M., Jolibois, J., Pons, J., Moreau, E., Touchard, G., Cazalens, M.: Optimization of a dielectric barrier discharge actuator by stationary and non-stationary measurements of the induced flow velocity: application to airflow control. Exp. Fluids **43**, 917 (2007)
11. Benard, N., Moreau, E.: Electrical and mechanical characteristics of surface AC dielectric barrier discharge plasma actuators applied to airflow control. Exp. Fluids **55**, 1846 (2014)
12. Yang, L., Yan, H.J., Qi, X.H., Hua, Y., Ren, C.S.: Airflow acceleration performance of asymmetric surface dielectric barrier discharge actuators at different exposed needle electrode heights. J. Appl. Phys. **118**, 223301 (2015)
13. Porter, C.O., Baughn, J.W., McLaughlin, T.E., Enloe, C.L., Font, G.I.: Temporal force measurements on an aerodynamic plasma

actuator. In: 44th AIAA Aerospace Sciences Meeting and Exhibit, Reno, Nevada, vol. 104, pp. 1–15 (2006)

14. Mahdavi, H., Sohbatzadeh, F.: The role of non-linear body force in production of the electric wind in an asymmetric surface dielectric barrier discharge. Phys. Scr. Accepted for publication. https://doi.org/10.1088/1402-4896/ab0e17

15. Moreau, E., Touchard, G.: Enhancing the mechanical efficiency of electric wind in corona discharges. J. Electrost. **66**, 39 (2008)

16. Corke, T.C., Post, M.L., Orlov, D.M.: SDBD plasma enhanced aerodynamics: concepts, optimization and applications. Prog. Aerosp. Sci. **43**, 193 (2007)

17. Thomas, F.O., Corke, T.C., Iqbal, M., Kozlov, A., Schatzman, D.: Optimization of dielectric barrier discharge plasma actuators for active aerodynamic flow control. AIAA J. **47**, 2169 (2009)

18. Font, G.I., Enloe, C.L., McLaughlin, T.E., Orlov, D.: Plasma discharge characteristics and experimentally determined boundary conditions for a plasma actuator. In: 45th AIAA Aerospace Sciences Meeting and Exhibit, Reno, Nevada, vol. 188, p. 1–14 (2007)

19. Enloe, C.L, McLaughlin, T.E., Gregory, J.W., Medina, R.A., Miller, W.S.: Surface potential and electric field structure in the aerodynamic plasma actuator. In: 46th AIAA Aerospace Sciences Meeting and Exhibit, Reno, NV, vol. 1103, pp. 1–11 (2008)

20. Nichols, T.G., Rovey, J.L.: Fundamental processes of DBD plasma actuators operating at high altitude. In: 50th AIAA Aerospace Sciences Meeting including the New Horizons Forum and Aerospace Exposition, Nashville, Tennessee, vol. 0822, pp. 1–23 (2012)

21. Cristofolini, A., Neretti, G., Borghi, C.A.: Effect of the charge surface distribution on the flow field induced by a dielectric barrier discharge actuator. J. Appl. Phys. **114**, 073303 (2013)

22. Yang, L., Yan, H.J., Qi, X.H., Hua, Y., Ren, C.S.: Surface potential distribution and airflow performance of different air-exposed electrode plasma actuators at different alternating current/direct current voltages. Phys. Plasmas **22**, 043518 (2015)

23. Benard, N., Moreau, E.: Role of the electric waveform supplying a dielectric barrier discharge plasma actuator. Appl. Phys. Lett. **100**, 193503 (2012)

24. Abe T., Takizawa, Y., Sato, S.: A parametric experimental study for momentum transfer by plasma actuator. In: 45th AIAA

Aerospace Sciences Meeting and Exhibit, Reno, Nevada, vol. 187, pp. 1–11 (2007)

25. Borghi, C.A., Cristofolini, A., Grandi, G., Neretti, G., Seri, P.: A plasma aerodynamic actuator supplied by a multilevel generator operating with different voltage waveforms. Plasma Sources Sci. Technol. **24**, 045018 (2015)

26. Opaits, D.F., Likhanskii, A.V., Neretti, G., Zaidi, S., Shneider, M.N., Miles, R.B., Macheret, S.O.: Experimental investigation of dielectric barrier discharge plasma actuators driven by repetitive high-voltage nanosecond pulses with dc or low frequency sinusoidal bias. J. Appl. Phys. **104**, 043304 (2008)

27. Yan, H., Yang, L., Qi, X., Ren, C.: Effect of a direct current bias on the electrohydrodynamic performance of a surface dielectric barrier discharge actuator for airflow control. J. Appl. Phys. **117**, 063302 (2015)

28. Roth, J. R., Dai, X.: Optimization of the aerodynamic plasma actuator as an electrohydrodynamic (EHD) electrical device. In: 44th AIAA Aerospace Sciences Meeting and Exhibit, Reno, Nevada, vol. 1203, pp. 1–28 (2006)

29. Opaits, D.F., Shneider, M.N., Miles, R.B., Likhanskii, A.V., Macheret, S.O.: Surface charge in dielectric barrier discharge plasma actuators. Phys. Plasmas **15**, 073505 (2008)

30. Opaits, D.F., Zaidi, S., Shneider, M.N., Miles, R.B., Likhanskii, A.V., Macheret, S.O.: Improving thrust by suppressing charge build-up in pulsed DBD plasma actuators. In: 47th AIAA Aerospace Sciences Meeting Including The New Horizons Forum and Aerospace Exposition, Orlando, Florida, vol. 487, pp. 1–8 (2009)

31. Guo, S., Burman, D., Poon, D., Mamunuru, M., Simon, T., Ernie, D., Kortshagen, U.: Separation control using DBD plasma actuators: designs for thrust enhancement. In: 39th AIAA Fluid Dynamics Conference San Antonio, Texas, p. 4184 (2009)